ORGANOMETALLICS

Article

pubs.acs.org/Organometallics

Use of the Imine−Enamine Equilibrium in Cooperative Ligand Design

Truman C. Wambach, Jun Myun Ahn, Brian O. Patrick, and Michael D. Fryzuk*

Department of Chemistry, The University of British Columbia, 2036 Main Mall, Vancouver, British Columbia, Canada V6T 1Z1

Supporting Information

ABSTRACT: The imine−phosphine ligands $Ph_2PC_5H_7NAr$, where Ar = 2,6-$Pr^i_2C_6H_3$, 2,6-$Me_2C_6H_3$, were deprotonated using KH to generate the corresponding potassium salts, which were reacted with $[(COD)IrCl]_2$ to generate the enamidophosphine derivatives $(COD)Ir(Ph_2PC_5H_6NAr)$ (Ar = 2,6-$Pr^i_2C_6H_3$, **4a**; Ar = 2,6-$Me_2C_6H_3$, **4b**). These complexes were exposed to alcohols, H_2, and CO to generate a series of products, some of which involve protonation of the enamido unit to generate the imine tautomer. The reaction of **4a** with isopropyl alcohol or H_2 generates the dinuclear hexahydride $[(Ph_2PC_5H_7N\text{-}2,6\text{-}Pr^i_2C_6H_3)IrH_2]_2(\mu\text{-}H)_2$ (**5a**), while the reaction with primary alcohols generates the dicarbonyl enamidophosphine complex $(CO)_2Ir(Ph_2PC_5H_6NAr)$ (**6a**). The reaction of the hexahydride **5a** with CO generates **6a**, for which a mechanism is proposed on the basis of monitoring this reaction as a function of time by NMR spectroscopy. On the basis of these experiments, cooperative ligand effects can be replicated by imine−phosphine ligands by proton transfer to and from the ligand backbone.

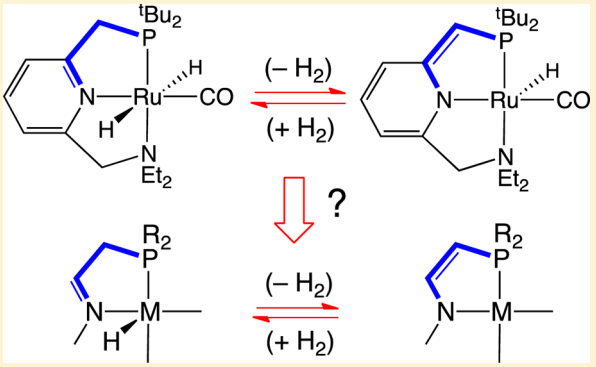

INTRODUCTION

When one designs a new ancillary ligand system to be used in concert with metal ions to generate potential catalyst precursors, a modular system wherein steric and electronic effects can be systematically varied has been de rigueur for decades. In addition, it has been assumed that the ancillary ligand should remain innocent and not participate in any of the elementary steps of the transformation of interest. However, recently a new paradigm has appeared in which it is desirable that the ligand system be able to cooperate during the transformation via a redox type reaction,[1−4] proton transfer steps,[5−26] or perhaps both. These cooperative ligand systems have shown remarkable results in a variety of processes, for example, the conversion of alcohols and amines to esters[6] and amides,[9] and even in the reverse reaction, in the hydrogenation of carbonyl functionalities.[7]

A particularly important example is the tridentate pyridine-based ligand system **1** in eq 1. In this case, it is the involvement

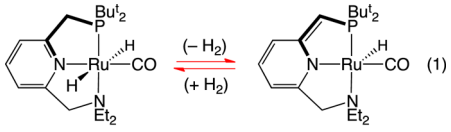

1

of a hydrogen from the ligand backbone with a ruthenium hydride that acts cooperatively to lose dihydrogen (H_2) and generate the dearomatized ligand framework that has been proposed to be involved in the catalytic dehydrogenation of reactions.[6,9]

We noticed that the equilibrium described in eq 1 could also be compared to the related equilibrium between complexes **A** and **B** in Scheme 1, in which the ligand scaffold is simplified to

Scheme 1

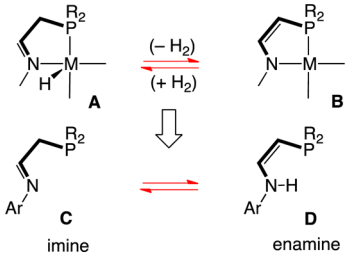

a bidentate metal imine−phosphine fragment **A** that could be in equilibrium with the metal-enamido moiety **B** and dihydrogen. We reasoned that these two species could be superficially related to the equilibrium between an imine and an enamine, as shown in **C** and **D** in Scheme 1. What becomes evident is that this kind of cooperativity between **A** and **B** does not necessarily require dearomatization/aromatization, as shown explicitly for **1** in eq 1; instead, one can also invoke participation of the linker between an imine and another donor such as a phosphine.[11,13−16,27−29]

In this report we examine the deprotonation and coordination chemistry of a simple imine−phosphine ligand with iridium(I) and its reactivity with small molecules in an

Received: July 13, 2013

   dx.doi.org/10.1021/om400688v | *Organometallics* XXXX, XXX, XXX−XXX

attempt to replicate transformations that would be consistent with ligand cooperativity.

RESULTS AND DISCUSSION

We chose to examine the known arylimine phosphine ligand systems **2a**,**b**, which were prepared according to modifications of literature procedures as shown in Scheme 2.[30,31] The short-

Scheme 2

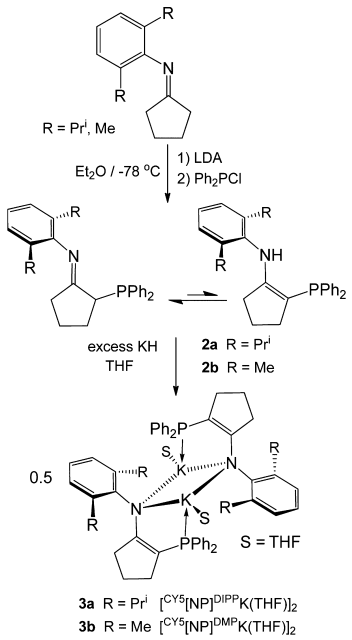

form descriptors we use are $^{CY5}[NP]^{DIPP}H$ (**2a**) and $^{CY5}[NP]^{DMP}H$ (**2b**), in which CY5 represents the cyclopentylidene linker and DIPP and DMP are 2,6-diisopropylphenyl and 2,6-dimethylphenyl, respectively, which are the imine N-aryl substituents. In solution both **2a**,**b** exist predominantly in the imine form, with the enamine tautomer evident by a small upfield peak in the $^{31}P\{^1H\}$ NMR spectrum.

Addition of excess KH in THF to solutions of **2a**,**b** results in the formation of the corresponding potassium salts **3a**,**b**, which can be isolated as solids in 68−78% yield. In solution, these species display singlets in the $^{31}P\{^1H\}$ NMR spectra at δ −22.7 and −19.1 for **3a**,**b**, respectively. The ^1H NMR spectra of both compounds are quite simple and show resonances that indicate that the alkyl substituents in the *ortho* positions of the *N*-aryl moiety are equivalent, as are the phenyl groups attached to the phosphine. A ^{13}C HSQC experiment displays a carbon signal at δ 69.2 with $^1J_{PC}$ = 14.8 Hz for **3a** that does not correlate to any resonance in the ^1H NMR spectrum, which is consistent with the α-carbon next to the PPh_2 unit in the deprotonated enamido structure; similar features in the NMR spectra are evident for **3b**. In the ^1H NMR spectrum of **3a** the resonances for the β-CH_2 protons of the coordinated THF are partially obscured by a doublet assigned to the methyl protons of the isopropyl groups of the *N*-aryl moiety at δ 1.4. Close inspection of the ^{13}C HSQC and ^{13}C APT spectra show a correlation with a CH_2 resonance in the carbon-13 spectrum at 24.7 ppm. The α-CH_2 protons of coordinated THF are clearly visible at 3.4 ppm in the ^1H NMR spectrum of **3a**. It is possible to remove the coordinated THF under high vacuum (see the Supporting Information).

X-ray-quality crystals of **3b** were obtained from THF by the addition of hexanes. The solid-state molecular structure is given in Figure 1 along with selected bond lengths and bond angles.

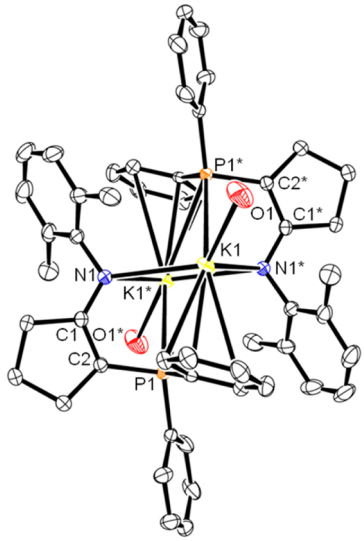

Figure 1. ORTEP drawing of the solid-state molecular structure of **3b**, with probability ellipsoids at the 50% level. The carbon atoms of both molecules of THF were excluded for clarity, as were all of the hydrogen atoms. Selected bond lengths (Å) and angles (deg): K1−O1 = 2.7050(18), K1−N1 = 2.9829(17), K1−N1* = 2.8222(17), K1−C12 = 3.066(2), K1−C17 = 3.216(2), K1−C24 = 3.280(3), K1−P1 = 3.4141(10), K1−K1* = 3.5045(13), N1−C1 = 1.347(2), C1−C2 = 1.347(2); N1−C1−C2 = 127.26(16), C1−C2−P1 = 120.46(10).

Overall, the structure is dimeric with the amido nitrogens of the enamido units bridging the two potassium ions, with one coordinated THF also bound to each potassium. One notable feature is that one of the phenyl rings attached to the phosphorus of the ligand participates in an η^3 interaction with the K^+. Due to this interaction the two phenyl rings attached to the phosphorus are not equivalent, and overall the compound is C_i symmetric in the solid state. As mentioned above, the observed inequivalent *P*-phenyl groups in the solid state are not maintained in solution.

Synthesis and Reactivity of Iridium Enamido Complexes. The reaction of the potassium derivatives **3a**,**b** with $[(COD)IrCl]_2$ at room temperature in toluene results in an immediate color change to produce a bright red solution along with the formation of potassium chloride. After workup, the pure iridium enamido complexes $^{CY5}[NP]^{DIPP}Ir(COD)$ (**4a**) and $^{CY5}[NP]^{DMP}Ir(COD)$ (**4b**) could be obtained in good yields. Similar bidentate ligands have been installed on iridium using salt methathesis.[32] Diagnostic of these complexes are the upfield-shifted singlets in the $^{31}P\{^1H\}$ NMR spectra, in comparison to the precursor potassium salts; for example, for **4a**, this resonance is observed at δ 12.1, whereas the signal for **3a** is found at δ −22.7.

Monitoring the reaction by $^{31}P\{^1H\}$ NMR spectroscopy shows that the formation of **4a**,**b** is quantitative and virtually instantaneous at the time of mixing. ^1H and ^{13}C NMR data and elemental analyses are consistent with the square-planar enamido complexes shown in eq 2.

X-ray-quality crystals of **4a** were obtained by allowing a hexanes solution of the complex to slowly evaporate or by cooling a concentrated hexanes solution to −35 °C. The

dx.doi.org/10.1021/om400688v | *Organometallics* XXXX, XXX, XXX−XXX

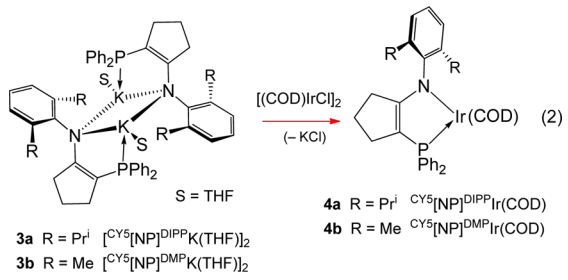

molecular structure is shown in Figure 2 along with selected bond lengths and bond angles.

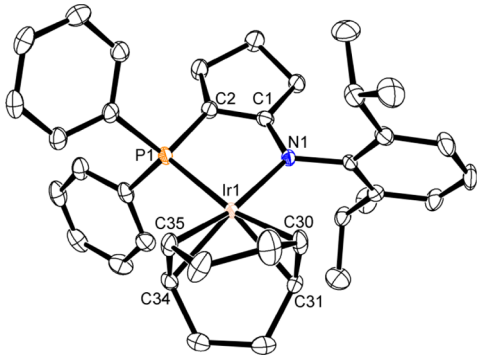

Figure 2. ORTEP drawing of the solid-state molecular structure of **4a** with probability ellipsoids at the 50% level. Selected bond lengths (Å) and angles (deg): Ir1−N1 = 2.061(2), Ir1−P1 = 2.3047(7), Ir1−C31 = 2.200(3), Ir1−C30 = 2.201(3), Ir1−C31 = 2.200(3), Ir1−C34 = 2.117(3), Ir1−C35 = 2.131(3), N1−C1 = 1.365(3), C1−C2 = 1.360(4), C2−P1 = 1.747(3), C30−C31 = 1.384(4), C34−C35 = 1.414(4); N1−C1−C2 = 124.6(3), C1−C2−P1 = 113.5(2), N1−Ir1−P1 = 81.12(6), C34−Ir1−P1 = 93.00(7), C35−Ir1−P1 = 96.55(8), N1−Ir1−C30 = 94.93(10), N1−Ir1−C31 = 97.86(10).

The geometry around iridium is square planar as expected, with the N1−C1−C2-P1 plane relatively flat and coplanar with the P1−Ir1−N1 plane. The Ir1−N1 bond length of 2.061(2) Å is similar to those in other iridium amido derivatives, and the Ir1−P1 distance of 2.3047(7) Å is typical. In addition the COD unit is bound normally, with the two double bonds perpendicular to the square plane of the complex.

In an effort to replicate typical transformations proposed for cooperative ligands, we examined the reactivity of the iridium enamido complexes with dihydrogen and with alcohols. Exposing **4a** to 4 atm of H_2 in pentane causes the solution to darken to a deep red-orange and is accompanied by the formation of a light yellow precipitate, which can be identified as the hexahydride dimer **5a**. A similar result occurs if the reaction of H_2 with **4a** is repeated in C_6D_6 in a J. Young NMR tube. Monitoring the reaction by $^{31}P\{^1H\}$ NMR spectroscopy shows that the reaction pathway is complex, as a number of unidentified intermediates are observed. Over a period of 12 h, the 1,5-cyclooctadiene ligand is completely hydrogenated to cyclooctane, as monitored by ^1H NMR spectroscopy (eq 3). In addition to a singlet due to **5a** at δ 32.7, two other unidentified signals are observed at δ 11.3 and −7.4. **5a** is easily separated from this mixture by washing with hexanes. Attempts to extend these results with **4b** resulted in intractable mixtures of products.

Treating a benzene solution of **4a** with excess isopropyl alcohol in a sealed reaction vessel and heating to 90 °C

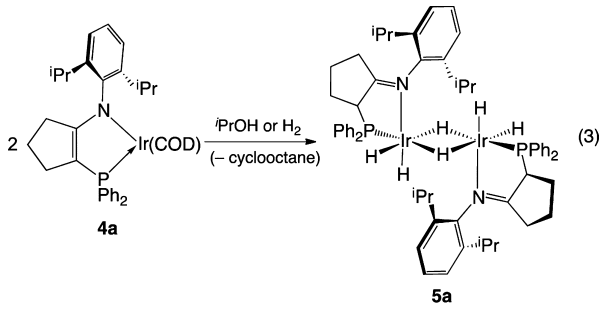

overnight also forms **5a**. If a J. Young tube is charged with 0.033 g of **4a**, 0.5 mL of C_6H_6, and 0.5 mL of isopropyl alcohol, clear, yellow, X-ray-quality crystals form upon heating overnight, which correspond to **5a** (Figure 3). Generally if the reaction is performed on a larger scale, a fine yellow powder is recovered in moderate yield.

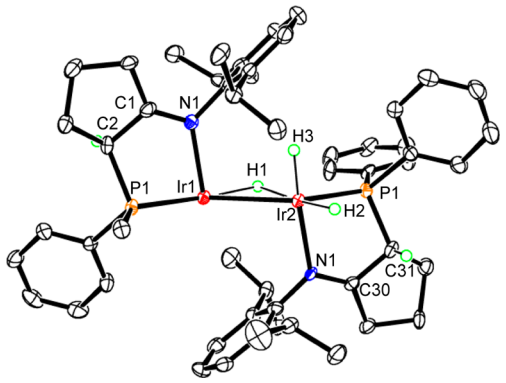

Figure 3. ORTEP drawing of the solid-state molecular structure of **5a** with probability ellipsoids at the 50% level. All of the hydrogen atoms except α-protons and hydrides have been excluded for clarity. One P1-phenyl has been removed for clarity. Three hydrides, H1, H2, and H3, were located from the difference map; their isotropic thermal parameters (U_{eq}) were coupled to Ir2, and their coordinates were freely refined. The X-ray data did not allow the remaining three hydrides to be located with any certainty. Selected bond lengths (Å) and angles (deg): Ir1−N1 = 2.238(9), Ir1−P1 = 2.210(3), Ir2−N2 = 2.236(8), Ir2−P2 = 2.196(3), Ir1−Ir2 = 2.7089(4), N1−C1 = 1.288(12), C1−C2 = 1.522(13), N2−C30 = 1.286(12), C30−C31 = 1.509(13); N1−C1−C2 = 120.9(9), P1−C2−C1 = 108.1(6), P1−Ir1−N1 = 81.3(2), P2−Ir2−N2 = 81.2(2).

Because **5a** is sparingly soluble in benzene, toluene, and other nonpolar organic solvents, acquiring multinuclear NMR spectra proved difficult. However, meaningful spectra could be obtained in CD_2Cl_2 even though the complex slowly decomposes in this solvent. Of particular importance to confirm the solid-state structure (Figure 3) was identification of the proton on the ancillary ligand for the imine tautomeric form of the ligand. The ^1H NMR spectrum taken at 600 MHz in CD_2Cl_2 shows a resonance at δ 3.7, which with ^{13}C APT and HSQC experiments indicates that this signal correlates to a CH carbon signal δ 62.8 (d, $^1J_{PC}$ = 33.1 Hz) strongly coupled to phosphorus, thus confirming that protonation at carbon has occurred. In the ^1H NMR spectrum all of the signals assigned to the various CH_2 groups of the cyclopentylidene linker appear as well-resolved diastereotopic multiplets, each integrating to one proton per iridium center. Additional information about the structure of **5a** was gleaned from the three unique signals in the hydride region of the spectrum, one of which is a triplet at δ

dx.doi.org/10.1021/om400688v | Organometallics XXXX, XXX, XXX−XXX

−20.0, which results from coupling to two equivalent phosphorus-31 nuclei and denotes that a dimeric structure exists in solution. When the ^{31}P nucleus is decoupled, the signal collapses into a broad singlet. We observe no H−H coupling between any of the three unique hydride signals. In solution, the overall symmetry of the dimer is C_i symmetric, which is identical with the symmetry observed in the solid state.

The solid-state molecular structure is shown in Figure 3, along with selected bond lengths and angles. All of the metrical parameters of the ligand are unremarkable and confirm protonation of the ligand at carbon. The iridium−iridium distance is 2.7089(4) Å, which is shorter than the sum of the van der Waals radius of the two atoms.[33] A similar compound with a tridentate ligand and a hemilabile arm has an iridium−iridium distance of 2.7325(7) Å and has been assigned as an iridium−iridium double bond.[34] Cationic iridium polyhydride clusters have been previously investigated, and their formation usually indicates catalyst deactivation during hydrogenation type processes.[35−39] Consistent with this is the fact that hexahydride **5a** does not react further with dihydrogen, with additional isopropyl alcohol, or even with primary alcohols such as benzyl alchohol (vide infra).

While speculative, one can propose a mechanism for the formation of this hexahydride dimer **5a** by reaction of **4a** with isopropyl alcohol, as shown in Scheme 3. The first step is

Scheme 3

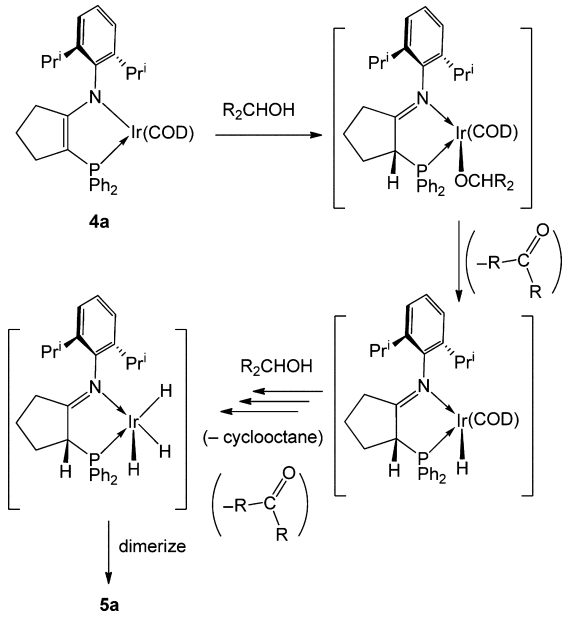

protonation of the enamido ligand to generate an imine phosphine derivative with a coordinated isopropoxy unit; subsequent β-elimination results in the formation of acetone and an Ir(I) hydride intermediate. Further reaction with more isopropyl alcohol in a multistep process results in the hydrogenation of the 1,5-cyclooctadiene and the formation of the imine−phosphine iridium(III) trihydride (Scheme 3).

When primary alcohols such as ethanol and benzyl alcohol are used in place of isopropyl alcohol, entirely different reactivity is observed (Scheme 4). Heating the iridium enamido compound **4a** dissolved in toluene in either an open reflux under nitrogen or a sealed reaction vessel results in the formation of a light red solution. Monitoring the reaction by

Scheme 4

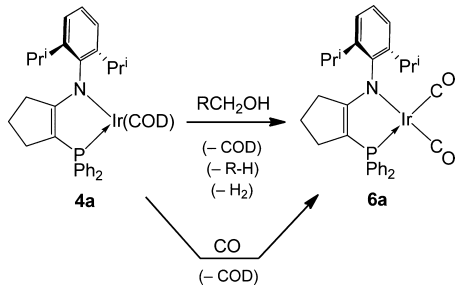

$^{31}P\{^1H\}$ NMR spectroscopy shows clean conversion of the singlet at δ 12.1 (**4a**) to a new signal at δ 21.3 that is assigned as the dicarbonyl complex **6a**. Removing the volatiles under vacuum gives a red oil that can be dissolved into C_6D_6 for characterization by multinuclear NMR spectroscopy.

The ^1H NMR spectrum of the red oil shows that the COD ligand has been lost; furthermore, no resonance diagnostic of protonation of the ligand can be found. ^{13}C APT and HSQC definitively establish that the ligand is in the enamido form, since the resonance for the carbon atom of the linker directly attached to phosphorus occurs at δ 83.5 (d, $^1J_{PC}$ = 64.4 Hz) and does not correlate with any signal in the ^1H NMR spectrum. No resonance attributable to an NH proton is observed. The CH_2 protons of the linker appear as three signals with the expected splitting patterns each integrating to two protons. Overall, the data point to a molecule with C_s symmetry in solution.

Confirmation of the presence of two different carbonyl ligands was given by ATR FTIR spectroscopy of a crystalline sample of the complex (Supporting Information). Two distinct CO stretches occur at 1966 and 2041 cm^{-1}.

Further evidence for the proposed structure was achieved by independently synthesizing **6a** by treating the COD complex **4a** with 1 atm of CO. Monitoring the reaction by $^{31}P\{^1H\}$ NMR spectroscopy shows that it quickly goes to completion, giving the expected singlet at δ 21.3; ^1H NMR spectroscopy confirms loss of the COD ligand. The reaction mixture was taken to dryness and subsequently dissolved in a minimal amount of hexanes. X-ray-quality crystals formed by slowly evaporating the hexanes from a loosely sealed vial overnight in a glovebox or by cooling a concentrated solution to −35 °C.

The solid-state molecular structure is shown in Figure 4, along with selected bond lengths and bond angles. As is clearly evident, **6a** is square planar as expected and matches the COD starting complex **4a** in terms of bond lengths and angles. Solution data and the solid-state molecular structure are consistent with each another. The oxidation of primary alcohols, followed by decarbonylation of the resulting aldehydes, has been documented for several late-transition-metal coordination compounds.[40−46] While we have not investigated the mechanism here, it is possibly very similar to that shown in Scheme 3, except that upon β-elimination of the primary alkoxy group the aldehyde produced can be oxidatively added and decarbonylated. At some stage, elimination of H_2 from an intermediate, perhaps cooperatively from the imine phosphine ligand and an iridium hydride, generates the enamido dicarbonyl derivative **6a**.

As shown by the reaction of alcohols with the iridium enamide derivative **4a**, different outcomes are observed depending on whether a primary versus a secondary alcohol

dx.doi.org/10.1021/om400688v | Organometallics XXXX, XXX, XXX−XXX

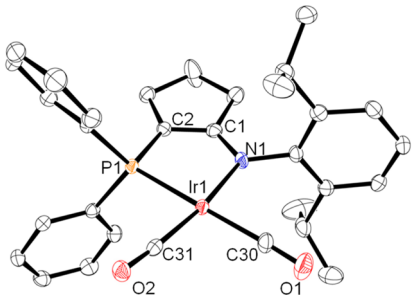

Figure 4. ORTEP drawing of the solid-state molecular structure of **6a** with probability ellipsoids at the 50% level. All of the hydrogen atoms have been removed for clarity. Selected bond lengths (Å) and angles (deg): Ir1−N1 = 2.047(2), Ir1−P1 = 2.3373(12), Ir1−C31 = 1.859(3), Ir1−C30 = 1.905(3), N1−C1 = 1.367(4), C1−C2 = 1.358(4), C2−P1 = 1.752(3); N1−C1−C2 = 125.0(2), C1−C2−P1 = 113.8(2), N1−Ir1−P1 = 82.26(7), C30−Ir1−N1 = 90.06(10), C31−Ir1−P1 = 90.05(8).

is used. As discussed above, we observe both the enamido and imine forms of the ligand in various complexes, which clearly indicates that the ligand is noninnocent in these transformations and is perhaps acting in a cooperative manner. To probe this further, we examined the reaction of the iridium(III) hexahydride dimer **5a** with CO and found that we could also generate the enamido dicarbonyl **6a** (eq 4).

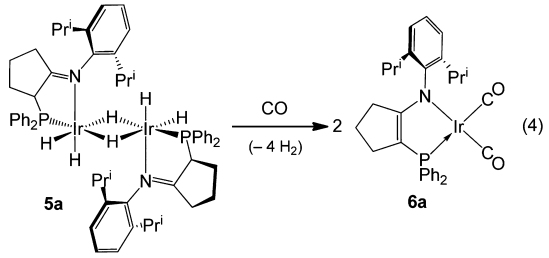

(4)

This is a slow reaction that takes a few days under 1 atm of CO and at 25 °C. As a result, we could observe intermediates by monitoring this process as a function of time by multinuclear NMR spectroscopy using natural-abundance CO and carbon-13 labeled CO. Suspending **5a** in d_8-THF in a J. Young or a flame-sealed NMR tube under slightly less than 1 atm of carbon monoxide resulted in the observation of three hydride intermediates, in varying amounts, on the way to **6a**. Interestingly, the same hydride complexes could be identified when more forcing conditions were used: for example, addition of 4 atm of CO at 60 °C. On the basis of the observation of these species, we propose the mechanism shown in Scheme 5, which tries to incorporate these observed species with other plausible intermediates on the basis of simple elementary reactions such oxidative addition and reductive elimination.

The first *observed* hydride intermediate is identified as **BB**, in which the imine donor is dissociated. The NMR data (see the Supporting Information) are consistent with this species containing three inequivalent hydrides, two inequivalent CO's, and one coordinated phosphine unit; the inequivalent hydrides are a result of the geometry as well as the presence of the chiral center on the imine backbone. With unlabeled CO, the hydrides appear as two overlapping doublets at δ −10.9 and −10.8 due to *cis* coupling to phosphorus-31 and a doublet at δ −11.2 with a large *trans* coupling to phosphorus-31. Use of ^{13}CO results in a doublet of triplets for the hydride *trans* to phosphorus and more complex but analyzable multiplets for the inequivalent *cis* hydrides. As shown in Scheme 5, a reasonable pathway for the formation of **BB** is addition of 1 equiv of CO to cleave the hydride dimer **5a** and generate the trihydride monocarbonyl **AA** (not observed), which upon dissociation of the bulky imine donor can be subsequently trapped by CO to generate **BB**.

The next observed intermediate is identified as **DD**, a square-planar, monohydride iridium(I) complex with the imine unit coordinated and only one carbonyl ligand. Its ^{31}P{^{1}H} resonance (δ 1.6, s) was assigned on the basis of correlations observed by ^{31}P HMBC as well as ^{1}H and ^{1}H{^{31}P} spectra. The hydride resonance for **DD** in the ^{1}H NMR spectrum (δ −11.6, d, $^2J_{PH}$ = 52.2 Hz) as well as the α-CH of the linker (δ 4.2, v dt, $^2J_{HH}$ = 7.7 Hz, $^2J_{PH}$ = 13.5 Hz) both show cross peaks to the ^{31}P{^{1}H} signal; interestingly, no coupling of the hydride to the *cis* ^{13}CO could be resolved. However, the ^{13}C HMBC spectrum confirms the presence of a CO ligand (δ 176.9, s) by correlation of this signal to the hydride resonance. The formation of **DD** could result via reductive elimination of H_2 from **BB** to form the dicarbonyl monohydride species **CC** (not observed), which upon associative binding of the imine followed by CO dissociation, or the reverse, results in the formation of **DD**.

The third hydride intermediate detected is **FF**, which corresponds to the ^{31}P{^{1}H} NMR singlet resonance at δ 30.6. The ^{31}P HMBC of the reaction using ^{13}C-labeled CO correlates this resonance to an NH resonance (6.0, s) and a hydride signal (δ −12.1, dq, $^2J_{PH}$ = 80.3 Hz, $^2J_{CH}$ = 5.3 Hz); the quartet pattern for the hydride is a result of coupling to three equivalent ^{13}CO ligands, which correspond to a resonance located in the ^{13}C APT NMR spectrum (δ 176.5, d, $^2J_{PC}$ = 8.5 Hz), and is confirmed by the ^{13}C HMBC data. The most important feature of **FF** is that the ligand is in the enamine form, bound only through the phosphine unit. We suggest that **FF** forms via the unobserved dicarbonyl **CC** by an imine-to-enamine tautomerism, followed by trapping with CO. We believe that this tautomerization (conversion of **CC** to **EE**) is a key step by which these imine−phosphine ligands can replicate cooperative ligand processes, as it provides a simple way for a proton from the ligand backbone to combine with a metal hydride. This is expanded on below.

As shown in eq 4 and detailed in Scheme 5, the CO-induced conversion of hexahydride **5a** to dicarbonyl **6a** requires loss of 2 equiv of H_2 per iridium center, where three of the hydrogen atoms come from the iridium hydrides and one hydrogen originates from the backbone of the ligand; it is worth noting that the starting imine unit in **5a** is converted to the enamido form in **6a**. We are unable to determine how the hydrogen from the ligand actually combines with a metal hydride by the experiments reported here, nevertheless, we can speculate on some of the possibilities, particularly as they relate to cooperativity.

The observation of **DD** and **FF** on the way to **6a** suggests that the imine must tautomerize to the enamine, and we suggest that the equilibrium between **CC** and **EE** in Scheme 5 can account for this, but it should be emphasized that, during the CO addition reaction to the hexahydride **5a**, no other intermediates after **FF** are observed. We were able to run the reaction backward by addition of H_2 to the dicarbonyl **6a**, whereupon a new intermediate can be observed that is not present during the excess CO reaction. This new species is identified as the dihydride dicarbonyl **GG** in Scheme 5, which

dx.doi.org/10.1021/om400688v | *Organometallics* XXXX, XXX, XXX−XXX

Scheme 5

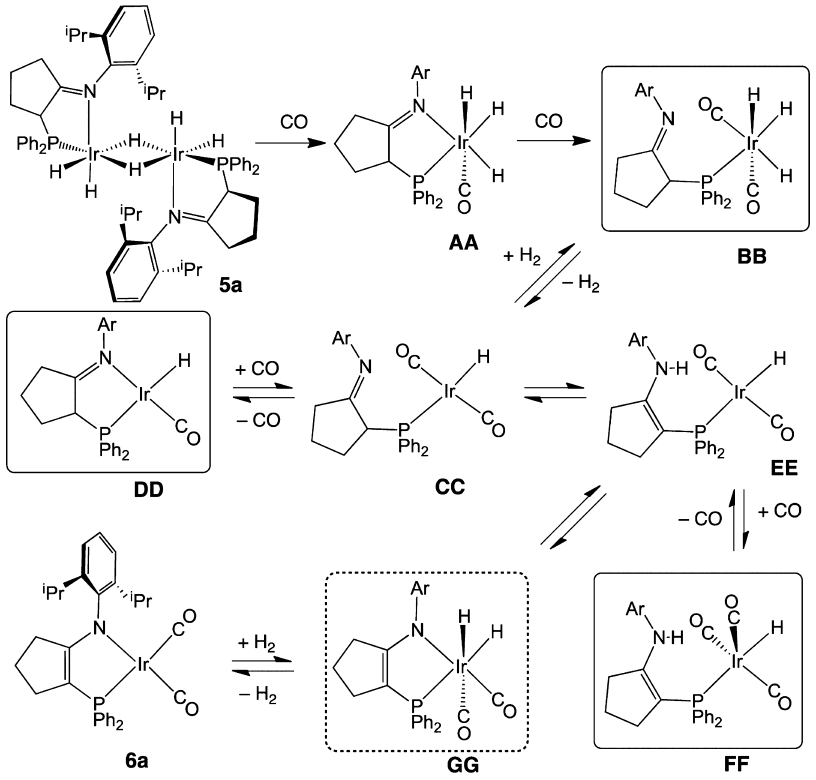

forms via *cis* oxidative addition of H_2 to **6a**. Particularly diagnostic of **GG** are the two doublet hydride resonances, one of which shows a large *trans* coupling to phosphorus ($^2J_{PH}$ = 123.0 Hz) and the other shows a smaller coupling indicative of being *cis* to the phosphine ($^2J_{PH}$ = 12.0 Hz); confirmation that **GG** has two carbonyl ligands is obtained by addition of H_2 to the ^{13}CO-labeled isotopologue of **6a**, which results in further multiplicities consistent with one CO *trans* to one of the hydrides and one CO *cis* to both hydrides (see the Supporting Information). Furthermore, running the reaction backward under excess H_2 for longer periods results in the depletion of **GG** and observation of **BB**, the imine trihydride, formed in the CO addition process discussed above. It is worth noting that the conversion of **GG** to **BB** also results in transfer of a hydrogen atom from the iridium center to the ligand.

CONCLUSIONS

The identification of ligand-based processes that might combine with fundamental steps in catalysis, namely oxidative addition and reductive elimination, is the subject of this study, which involves a simple bidentate imine−phosphine ligand and its coordination chemistry and reactivity with iridium. While none of the alcohol dehydrogenations reported herein are catalytic, by examination of some simple reactions we find evidence to support that a hydrogen atom from the ligand backbone can combine with an iridium hydride to generate dihydrogen, and conversely a hydride on iridium can be transferred to the ligand. How this occurs is still a matter of conjecture, although it has been examined computationally for Ir, Ru, and Fe systems.[28,47−53] In our study we suggest without proof that this process results via oxidative addition of a dissociated enamine to generate an enamido hydride, shown in Scheme 5 as the equilibrium between **EE** and **GG**, respectively, which provides the key connection to relay the ligand proton to the iridium to ultimately form H_2. While the potentially bidentate imine−phosphine ligand coordinated to iridium examined here allows these steps to be inferred, it is clear that in relation to tridentate and even tetradentate systems that involve imines, pyridine, and phosphines, these bidentate systems would be less stable, especially under more harsh conditions typically found in catalytic processes that involve dehydrogenation. As we will report in due course, our bidentate systems can be made catalytic but their thermal instability makes them less efficient in comparison to the tridentate Milstein systems or the tetradentate Morris complexes.

EXPERIMENTAL PROCEDURES

General Considerations. All procedures and manipulations were performed under an atmosphere of dry, oxygen-free dinitrogen or argon by means of standard Schlenk or glovebox techniques. Argon and dinitrogen were dried and deoxygenated by passing the gases through a column containing molecular sieves and MnO. Hexanes, toluene, THF, and diethyl ether were purchased from Aldrich, dried by passage through a tower of alumina, and degassed by passage through a tower of Q-5 catalyst under positive pressure of nitrogen. ^{13}CO was purchased from Cambridge Isotope Laboratories in 1 L glass bulbs. Deuterated toluene, benzene, and THF were refluxed over sodium/benzophenone, trap-to-trap distilled, and freeze−pump−thaw degassed three times. Deuterated dichloromethane was purchased in ampules from Aldrich and used as received. ATR (attenuated total reflectance) FTIR (Fourier transform infrared spectroscopy) spectra were recorded on a Perkin-Elmer Frontier FTIR spectrometer. NMR (nuclear magnetic resonance) spectra were recorded on Bruker AvanceII 300 MHz and Bruker Avance 400 MHz spectrometers unless otherwise noted. Chemical shifts for ^{31}P nuclei were referenced to 85% H_3PO_4 in H_2O (0 ppm). ^{1}H nuclei were referenced to resonances of the residual protonated solvents relative to tetramethylsilane (0 ppm), and ^{13}C spectra were referenced to the solvent carbon resonance(s). Elemental analysis was performed at the facilities of the Chemistry Department of the University of British Columbia.

dx.doi.org/10.1021/om400688v | *Organometallics* XXXX, XXX, XXX−XXX

Caution! All reactions that resulted in a pressure of 1.5 atm or greater within a sealed vessel upon warming to room temperature were performed with great care and were always manipulated behind a blast shield. Pressurized NMR tubes were warmed to room temperature in a safe location and used normally after.

$[(COD)IrCl]_2$[54] and **2a**,**b** were synthesized via literature procedures.[30,31] Isopropyl alcohol was dried over sodium and distilled into a Kontes-sealed thick-walled flask under nitrogen. Absolute ethanol and benzyl alcohol were degassed by purging with nitrogen. Potassium hydride was purchased from Aldrich as a suspension in oil. Using standard Schlenk techniques, the solid was collected on a glass frit, washed with hexanes, and dried under vacuum.

Synthesis of $[^{CY5}(NP)^{DIPP}K(THF)]_2$ (3a). In a Schlenk flask **2a** (8.83 g, 20.7 mmol) was added to excess potassium hydride (1.86 g, 46.4 mmol). THF (100 mL) was added, and the suspension was stirred overnight. During this time the solution became bright yellow. Small bubbles were observed. The reaction mixture was filtered through Celite. The solvent was removed by vacuum, which produced a yellow oil. It was triturated with pentane or hexanes. A pure yellow powder was collected by filtration through a glass frit (8.73 g, 78.6%). $^{31}P\{^1H\}$ NMR (C_6D_6, 161.9 MHz, 298 K): δ −19.1 (s). ^1H NMR (C_6D_6, 400.0 MHz, 298 K): δ 1.1 (d, 6H, $^3J_{HH}$ = 6.9 Hz, *N*-Pr^{i}CH$_3$), 1.4 (m, 4H, *THF*-CH$_2$), 1.4 (d, 6H, $^3J_{HH}$ = 6.8 Hz, *N*-Pr^{i}CH$_3$), 1.9 (m, 2H, γ-CH$_2$), 2.3 (t, 2H, $^3J_{HH}$ = 7.3 Hz, β-CH$_2$), 2.7 (t, 2H, $^3J_{HH}$ = 6.6 Hz, δ-CH$_2$), 3.4 (m, 4H, *THF*-CH$_2$), 3.5 (m, 2H, *N*-Pr^{i}CH) 7.0 (t, 1H, $^3J_{HH}$ = 7.5 Hz, *N*-*p*-ArCH), 7.1 (m, 4H, *N*-*m*/*P*-*p*-ArCH), 7.2 (v.t, 4H, *J* = 7.3 Hz, *P*-*m*-ArCH), 7.7 (v t, 4H, *J* = 7.2 Hz, *P*-*o*-ArCH). ^{13}C APT NMR (C_6D_6, 100.6 MHz, 298 K): δ 24.3 (s, *N*-Pr^{i}CH$_3$), 24.6 (s, γ-CH$_2$), 24.7 (s, *N*-Pr^{i}CH), 25.7 (s, *THF*-CH$_2$), 27.8 (s, *N*- Pr^{i}CH$_3$), 32.2 (d, $^2J_{PC}$ = 4.6, β-CH$_2$), 35.8 (d, $^3J_{PC}$ = 9.0, δ-CH$_2$), 67.8 (s, *THF*-CH$_2$), 69.2 (d, $^1J_{PC}$ = 14.8 Hz, α-C), 120.1 (s, *N*-*p*-ArCH), 123.2 (s, *N*-*m*-ArCH), 127.1 (s, *P*-*p*-ArCH), 128.4 (d, $^3J_{PC}$ = 6.1 Hz, *P*-*m*-ArCH), 133.2 (d, $^2J_{PC}$ = 16.4 Hz, *P*-*o*-ArCH) 142.2 (s, *N*-ArCPr^i), 142.4 (d, $^2J_{PC}$ = 3.1 Hz, *N*-C$_{enamide}$), 154.4 (s, *N*-CAr), 175.8 (d, $^1J_{PC}$ = 32.7 Hz, *P*-CAr). Anal. Calcd for $C_{33}H_{41}KNOP$: C, 73.70; H, 7.68; N, 2.60. Found: C, 73.64; H, 7.92; N, 2.99.

Synthesis of $[^{CY5}(NP)^{DMP}K(THF)]_2$ (3b). See the procedure for **3a**. After the yellow product was collected by filtration, the solution was concentrated and treated with hexanes. X-ray-quality crystals grew (performed on a variety of scales, yield 68.0%). The coordinated THF can be removed under high vacuum; see the Supporting Information for the relevant spectra. The THF adduct is described here. $^{31}P\{^1H\}$ NMR (C_6D_6, 161.9 MHz, 298 K): δ −22.1 (s). ^1H NMR (C_6D_6, 400.0 MHz, 298 K): δ 1.4 (m, 4H, *THF*-CH$_2$), 1.9 (m, 2H, γ-CH$_2$), 2.0 (s, 6H, *N*-CH$_3$), 2.2 (t, 2H, $^3J_{HH}$ = 7.5 Hz, δ-CH$_2$), 2.6 (t, 2H, $^3J_{HH}$ = 6.7 Hz, β-CH$_2$), 3.5 (m, 4H, *THF*-CH$_2$), 6.9 (t, 1H, $^3J_{HH}$ = 7.4 Hz, *N*-*p*-ArCH), 7.1 (d, 2H, $^3J_{HH}$ = 7.4 Hz, *N*-*m*-ArCH), 7.2 (t, 2H, $^3J_{HH}$ = 7.3 Hz, *P*-*p*-ArCH), 7.3 (v.t, 4H, *J* = 7.2 Hz, *P*-*m*-ArCH), 7.5 (v.t, 4H, *J* = 7.3 Hz, *P*-*o*-ArCH). ^{13}C APT NMR (C_6D_6, 100.6 MHz, 298 K): δ 20.0 (s, *N*-CH$_3$), 24.2 (d, $^2J_{PC}$ = 4.4 Hz, γ-CH$_2$), 25.7 (s, *THF*-CH$_2$), 32.5 (d, $^3J_{PC}$ = 4.8 Hz, δ-CH$_2$), 36.1 (d, $^3J_{PC}$ = 7.9 Hz, γ-CH$_2$), 67.8 (s, *THF*-CH$_2$), 69.9 (d, $^1J_{PC}$ = 9.8 Hz, α-C), 120.0 (s, *N*-*p*-ArCH), 127.3 (s, *P*-*p*-ArCH), 128.4 (d, $^3J_{PC}$ = 6.4 Hz, *P*-*m*-ArCH), 128.7 (s, *N*-*m*-ArCH), 131.6 (s, *N*-ArCMe), 133.4 (d, $^2J_{PC}$ = 16.9 Hz, *P*-*o*-ArCH), 141.6 (d, $^2J_{PC}$ = 3.3 Hz, *N*-C$_{enamide}$), 156.9 (s, *N*-CAr), 175.9 (d, $^1J_{PC}$ = 32.4 Hz, *P*-CAr). Anal. Calcd for $C_{29}H_{33}KNOP$: C, 72.23; H, 6.91; N, 2.91. Found: C, 71.43; H, 6.53; N, 3.76. Despite many attempts, satisfactory microanalyses could not be obtained.

Synthesis of $^{CY5}(NP)^{DIPP}Ir(COD)$ (4a). $[(COD)IrCl]_2$ (0.881 g, 1.31 mmol) was combined with **3a** (1.41 g, 1.31 mmol) in toluene (50 mL), and the mixture was stirred for about 20 min. The solution became an intense red, and a white precipitate (potassium chloride) formed, which was removed by Celite filtration. The solvent was removed, and the product was dried under vacuum to give a bright red solid. Recrystallization by slowly evaporating hexanes or cooling a concentrated hexanes solution to −35 °C gave X-ray-quality crystals (1.29 g, 67.5%). This reaction was performed on various scales. Conversion is quantitative by $^{31}P\{^1H\}$ and ^1H NMR spectroscopy. $^{31}P\{^1H\}$ NMR (C_6D_6, 161.9 MHz, 298 K): δ 12.1 (s). ^1H NMR (C_6D_6, 400 MHz, 298 K): δ 1.3 (d, 6H, $^3J_{HH}$ = 6.8 Hz, *N*-Pr^{i}CH$_3$), 1.5 (d, 6H, $^3J_{HH}$ = 6.9 Hz, *N*-Pr^{i}CH$_3$), 1.5 (m, 2H, *COD*-CH$_2$), 1.7 (m, 2H, *COD*-CH$_2$), 2.1 (m, 8H, γ-CH$_2$, 2 × *COD*-CH$_2$, β-CH$_2$), 2.4 (t, 2H, $^3J_{HH}$ = 6.5 Hz, δ-CH$_2$), 3.3 (br. d, 2H, J_{HH} = 2.7 Hz, *trans*-*N*-*COD*-CH), 4.0 (m, 2H, *N*-Pr^{i}CH), 4.1 (m, 2H, *trans*-*P*-*COD*-CH), 7.0−7.1 (m, 2H, *P*-*p*-ArCH), 7.1−7.2 (m, 5H, *N*-*p*/*P*-*m*-ArCH), 7.2 (m, 2H, *N*-*m*-ArCH), 7.8 (m, 4H, *P*-*o*-ArCH). ^{13}C APT NMR (C_6D_6, 100.6 MHz, 298 K): δ 24.5 (s, *N*-Pr^{i}CH$_3$), 25.6 (s, δ-CH$_2$), 25.6 (s, *N*-Pr^{i}CH$_3$), 27.8 (s, *N*-Pr^{i}CH), 28.7 (d, $^2J_{PC}$ = 8.7 Hz, β-CH$_2$), 30.1 (d, $^3J_{PC}$ = 1.2 Hz, *COD*-CH$_2$), 32.1 (d, $^3J_{PC}$ = 16.8 Hz, γ-CH$_2$), 33.0 (d, J_{PC} = 3.2 Hz, *COD*-CH$_2$), 53.9 (s, *trans*-*N*-*COD*-CH), 87.7 (d, $^1J_{PC}$ = 61.0 Hz, α-C), 90.2 (d, J_{PC} = 12.8 Hz, *trans*-*P*-*COD*-CH), 123.6 (s, *N*-*m*-ArCH), 125.7 (s, *N*-*p*-ArCH), 128.7 (d, $^3J_{PC}$ = 10.0 Hz, *P*-*m*-ArCH), 129.9 (d, $^3J_{PC}$ = 1.8 Hz, *P*-*p*-ArCH), 133.0 (d, $^2J_{PC}$ = 11.0 Hz, *P*-*o*-ArCH), 134.5 (d, $^2J_{PC}$ = 52.5 Hz, *N*-C$_{enamide}$), 145.2 (s, *N*-ArCPr^i), 147.9 (s, *N*-CAr), 189.9 (d, $^1J_{PC}$ = 32.3 Hz, *P*-CAr). Anal. Calcd for $C_{37}H_{46}IrNP$: C, 61.05; H, 6.34; N, 1.92. Found: C, 61.24; H, 6.15; N, 1.91.

Synthesis of $^{CY5}(NP)^{DMP}Ir(COD)$ (4b). See the procedure for **4a** (performed on a variety of scales, 57.0%). $^{31}P\{^1H\}$ NMR (C_6D_6, 161.9 MHz, 298 K): δ 11.5 (s). ^1H NMR (C_6D_6, 400 MHz, 298 K): δ 1.6 (m, 2H, *COD*-CH$_2$), 1.8 (m, 2H *COD*-CH$_2$), 2.0 (m, 2H, β-CH$_2$), 2.1 (m, 2H, *COD*-CH$_2$), 2.2 (m, 2H, *COD*-CH$_2$), 2.3 (m, 2H, γ-CH$_2$), 2.5 (t, 2H, $^3J_{HH}$ = 6.7 Hz, δ-CH$_2$), 2.7 (s, 6H, *N*-CH$_3$), 3.4 (dd, 2H, *J* = 2.7 Hz, *J* = 5.6 Hz, *trans*-*N*-*COD*-CH), 4.1 (dd, 2H, *J* = 2.6 Hz, *J* = 6.2 Hz, *trans*-*P*-*COD*-CH), 7.1 (t, 1H, $^3J_{HH}$ = 7.5 Hz, *N*-*p*-ArCH), 7.2 (m, 2H, *P*-*p*-ArCH), 7.2−7.3 (m, 6H, *N*-*m*-/*P*-*m*-ArCH), 7.9 (ddd, 4H, *J* = 1.1 Hz, *J* = 8.0 Hz, *J* = 9.6 Hz, *P*-*o*-ArCH). ^{13}C APT NMR (C_6D_6, 100.6 MHz, 298 K): δ 19.1 (s, *N*-CH$_3$), 25.4 (s, δ-CH$_2$), 28.2 (d, $^3J_{PC}$ = 9.1 Hz, γ-CH$_2$), 30.5 (d, J_{PC} = 2.0 Hz, *COD*-CH$_2$), 30.9 (d, $^2J_{PC}$ = 17.2 Hz, β-CH$_2$), 33.1 (d, J_{PC} = 3.4 Hz, *COD*-CH$_2$), 54.0 (s, *trans*-*N*-*COD*-CH), 87.5 (d, $^1J_{PC}$ = 60.8 Hz, α-C), 90.0 (d, J_{PC} = 12.8 Hz, *trans*-*P*-*COD*-CH), 124.7 (s, *N*-*p*-ArCH), 128.1 (s, *N*-*m*-ArCH), 128.8 (d, $^3J_{PC}$ = 10.0 Hz, *P*-*m*-ArCH), 129.0 (d, $^4J_{PC}$ = 2.2 Hz, *P*-*p*-ArCH), 133.0 (d, $^2J_{PC}$ = 11.1 Hz, *P*-*o*-ArCH), 134.4 (d, $^2J_{PC}$ = 52.0 Hz, *N*-C$_{enamide}$), 135.2 (s, *N*-ArMe), 150.6 (s, *N*-CAr), 188.6 (d, $^1J_{PC}$ = 32.6 Hz, *P*-CAr).

Synthesis of $[\{^{CY5}(NP)^{DIPP}\}Ir(H)_3]_2$ (5a). **4a** (0.405 g, 0.557 mmol) was dissolved in toluene (30 mL) in a Kontes sealed reaction flask. Isopropyl alcohol (30 mL) was added; the bomb (80 mL) was sealed and heated to 100 °C overnight. A yellow precipitate formed. The precipitate was allowed to settle, and the reaction mixture was decanted. It was washed with hexanes and taken to dryness to give a yellow solid (0.192 g, 55.2%). Alternatively, a J. Young tube was charged with **4a** (0.033 g), C_6H_6 (0.5 mL), and isopropyl alcohol (0.5 mL); clear, yellow, X-ray-quality crystals formed upon heating to 90 °C overnight. Alternatively, a Kontes sealed vessel charged with **4a** and toluene was freeze−pump−thaw degassed three times and back-filled with H_2 at −196 °C. The flask was sealed and warmed to room temperature under 4 atm of H_2. After the mixture was stirred overnight, the H_2 pressure was released and the mixture was taken to dryness. Addition of pentane, followed by filtration of the resulting suspension, allowed for the isolation of the desired product as a yellow solid. $^{31}P\{^1H\}$ NMR (d_2-DCM, 161 MHz, 298 K): δ 32.7 (s). ^1H NMR (d_2-DCM, 400 MHz, 298 K): δ −23.2 (v.dd, $^2J_{PH}$ = 8.6 Hz, $^2J_{HH}$ = 3.7 Hz, 2H, *trans*-*H*-*Ir*-H), −20.0 (t, $^2J_{PH}$ = 28.6 Hz, 2H, *bridging*-*Ir*-H), −8.6 (d, $^2J_{PH}$ = 82.9 Hz, 2H, *trans*-*N*-*Ir*-H), 0.81 (d, 6H, $^3J_{HH}$ = 6.7 Hz, *N*-Pr^{i}CH$_3$), 0.9 (d, 6H, $^3J_{HH}$ = 8.5 Hz, *N*-Pr^{i}CH$_3$), 0.9(2) (d, 6H, $^3J_{HH}$ = 7.1 Hz, *N*-Pr^{i}CH$_3$), 1.3 (m, 2H, δ-CH$_2$), 1.5 (d, 6H, $^3J_{HH}$ = 6.5 Hz, *N*-Pr^{i}CH$_3$), 1.7 (m, 2H, γ-CH$_2$), 1.8 (m, 2H, γ-CH$_2$), 1.9 (m, 2H, β-CH$_2$), 2.0 (m, 2H, β-CH$_2$), 2.3 (m, 2H, δ-CH$_2$), 2.8 (m, 2H, $^3J_{HH}$ = 6.5 Hz, *N*-Pr^{i}CH), 3.4 (m, 2H, $^3J_{HH}$ = 6.7 Hz, *N*-Pr^{i}CH), 3.7 (v.dt, 2H $^3J_{PH}$ = 9.5 Hz, $^3J_{HH}$ = 11.3 Hz, α-CH), 6.9 (d, 2H, $^3J_{HH}$ = 7.2 Hz, *N*-*m*-ArCH), 7.1 (t, 2H, $^3J_{HH}$ = 7.5 Hz, *N*-*p*-ArCH), 7.2 (d, 2H, $^3J_{HH}$ = 6.1 Hz, *N*-*m*-ArCH), 7.3 (m, 6H, *P*-*m*/*p*-ArCH), 7.4 (br.s, 6H, *P*-*m*/*p*-ArCH), 7.5 (br.m, 4H, *P*-*o*-ArCH), 7.8 (m, 4H, *P*-*o*-ArCH). ^{13}C APT NMR (d_2-DCM, 241.7 MHz, 298 K): δ 23.2 (s, *N*-Pr^{i}CH$_3$), 24.6 (s, *N*-Pr^{i}CH$_3$), 24.7 (s, *N*-Pr^{i}CH$_3$), 25.2 (s, *N*-Pr^{i}CH$_3$), 27.6 (d, $^2J_{PC}$ = 7.4 Hz, β-CH$_2$), 27.9 (s, *N*-Pr^{i}CH), 28.1 (s, *N*-Pr^{i}CH), 28.2 (d, $^3J_{PC}$ = 5.6 Hz, δ-CH$_2$), 31.2 (d, $^3J_{PC}$ = 6.3 Hz, γ-CH$_2$), 62.8 (d, $^1J_{PC}$ = 33.1 Hz, α-CH), 123.6 (s, *N*-*m*-ArCH), 123.7 (s, *N*-*m*-ArCH), 125.2 (s, *N*-*p*-ArCH), 127.8 (d, $^3J_{PC}$ = 9.7 Hz, *P*-*m*-ArCH), 128.1 (d, $^3J_{PC}$ = 10.4 Hz,

dx.doi.org/10.1021/om400688v | *Organometallics* XXXX, XXX, XXX−XXX

P-m-ArCH), 129.6(7) (d, $^4J_{PC}$ = 1.3 Hz, *P-p*-ArCH), 129.7(2) (d, $^4J_{PC}$ = 1.2 Hz, *P-p*-ArCH), 131.0 (d, $^1J_{PC}$ = 34.0 Hz, *P*-CAr), 133.7 (d, $^2J_{PC}$ = 11.4 Hz, *P-o*-ArCH), 134.5 (d, $^2J_{PC}$ = 13.1 Hz, *P-o*-ArCH), 138.6 (d, $^1J_{PC}$ = 61.3 Hz, *P*-ArC), 139.1 (s, *N*-ArCPr^i), 140.0, (s, *N*-ArCPr^i), 149.6 (s, *N*-Ar). A peak corresponding to $C_{enamide}$ could not be identified from −20 to 200 ppm in the ^{13}C APT spectrum. Anal. Calcd for $C_{29}H_{37}IrNP$: C, 55.93; H, 5.99; N, 2.25. Found: C, 56.05; H, 5.93; N, 2.63.

Synthesis of ^{CY5}(NP)^{DIPP}Ir(CO)$_2$ (6a). **4a** (0.250 g, 0.344 mmol) was dissolved in hexanes (30 mL) and transferred to a Kontes sealed vessel. The mixture was degassed with three freeze−pump−thaw cycles and warmed to room temperature under vacuum. CO was backfilled into the evacuated vessel. The solution instantly lightened. After the mixture was stirred for approximately 30 min, it was taken to dryness. The mixture was then dissolved in a minimal amount of hexanes and left to crystallize at −35 °C. X-ray-quality crystals formed (0.145 g, 63.0%). ^{31}P{^{1}H} NMR (C_6D_6, 161.9 MHz, 298 K): δ −21.3 (s). ^{1}H NMR (C_6D_6, 400.0 MHz, 298 K): δ 1.2 (d, 6H, $^3J_{HH}$ = 6.9 Hz, *N*-Pr^{i}CH$_3$), 1.4 (d, 6H, $^3J_{HH}$ = 6.8 Hz, *N*-Pr^{i}CH$_3$), 2.0 (t, 2H, $^3J_{HH}$ = 7.3 Hz, γ-CH$_2$), 2.2 (m, 2H, δ-CH$_2$), 2.4 (t, 2H, $^3J_{HH}$ = 6.6 Hz, β-CH$_2$), 3.9 (hept, 2H, $^3J_{HH}$ = 6.8 Hz, *N*-Pr^{i}CH), 7.0−7.1(m, 9H, ArCH), 7.8 (ddd, $^3J_{PC}$ = 12.2 Hz, $^3J_{HH}$ = 7.7 Hz, $^4J_{HH}$ = 1.7 Hz, *P-o*-ArCH). ^{13}C APT NMR (C_6D_6, 100.6 MHz, 298 K): δ 24.2 (s, Pr^{i}CH$_3$), 24.3(s, Pr^{i}CH$_3$), 26.4 (s, β-CH$_2$), 28.2 (s, Pr^{i}CH), 29.6 (d, $^3J_{PC}$ = 9.2 Hz, δ-CH$_2$), 31.3 (d, $^3J_{PC}$ = 17.7 Hz, γ-CH$_2$), 83.5 (d, $^1J_{PC}$ = 64.4 Hz, α-C), 123.4 (s, *N-m*-ArCH), 126.4 (s, *N-p*-ArCH), 129.2 (d, $^3J_{PC}$ = 11.0 Hz, *P-m*-Ar−CH), 130.9 (s, *P-p*-ArCH), 132.5 (s, *N*-ArC$_{enamide}$), 133.0 (d, $^2J_{PC}$ = 11.6 Hz, *P-o*-ArCH), 144.0 (s, *N*-CArPr^i), 152.5 (s, *N*-CAr), 180.1(d, $^2J_{PC}$ = 11.1 Hz, *trans-N*-CO), 181.5 (d, $^2J_{PC}$ = 103.5 Hz, *trans-P*-CO), 189.3 (d, $^1J_{PC}$ = 32.5 Hz, *P*-CAr). Anal. Calcd for $C_{31}H_{34}IrNO_2P$: C, 55.10; H, 5.07; N, 2.07. Found: C, 54.35; H, 4.89; N, 2.33. ATR FTIR: CO stretches occur at 1966 and 2041 cm^{-1}.

■ ASSOCIATED CONTENT

Supporting Information

Text, tables, figures, and CIF files giving crystallographic data and details of the X-ray structure refinement, pictures and full assignment of all the relevant multinuclear NMR spectra, and additional experimental details. This material is available free of charge via the Internet at http://pubs.acs.org.

■ AUTHOR INFORMATION

Notes

The authors declare no competing financial interest.

■ ACKNOWLEDGMENTS

We thank the NSERC of Canada for funding (Discovery Grant to M.D.F.). We also thank Nathan Halcovitch, Fraser Pick, and Dr. Brian O. Patrick for help with the X-ray structures.

■ REFERENCES

(1) Bart, S. C.; Chłopek, K.; Bill, E.; Bouwkamp, M. W.; Lobkovsky, E.; Neese, F.; Wieghardt, K.; Chirik, P. J. *J. Am. Chem. Soc.* **2006**, *128*, 13901.
(2) Bouwkamp, M. W.; Bowman, A. C.; Lobkovsky, E.; Chirik, P. J. *J. Am. Chem. Soc.* **2006**, *128*, 13340.
(3) Sylvester, K. T.; Chirik, P. J. *J. Am. Chem. Soc.* **2009**, *131*, 8772.
(4) Russel, S. K.; Milsmann, C.; Lobkovsky, E.; Weyhermuller, T.; Chirik, P. J. *Inorg. Chem.* **2011**, *50*, 3159.
(5) Zhang, J.; Gandelman, M.; Shimon, L. J. W.; Rozenberg, H.; Milstein, D. *Organometallics* **2004**, *23*, 4026.
(6) Zhang, J.; Leitus, G.; Ben-David, Y.; Milstein, D. *J. Am. Chem. Soc.* **2005**, *127*, 10840.
(7) Zhang, J.; Leitus, G.; Ben-David, Y.; Milstein, D. *Angew. Chem., Int. Ed.* **2006**, *45*, 1113.
(8) Ben-Ari, E.; Leitus, G.; Shimon, L. J. W.; Milstein, D. *J. Am. Chem. Soc.* **2006**, *128*, 15390.
(9) Gunanathan, C.; Ben-David, Y.; Milstein, D. *Science* **2007**, *317*, 790.
(10) Iron, M. A.; Ben-Ari, E.; Cohen, R.; Milstein, D. *Dalton Trans.* **2009**, 9433.
(11) Friedrich, A.; Ghosh, R.; Kolb, R.; Herdtweck, E.; Schneider, S. *Organometallics* **2009**, *28*, 708.
(12) Schwartsburd, L.; Iron, M. a.; Konstantinovski, L.; Diskin-Posner, Y.; Leitus, G.; Shimon, L. J. W.; Milstein, D. *Organometallics* **2010**, *29*, 3817.
(13) Friedrich, A.; Drees, M.; Schmedt auf der Günne, J.; Schneider, S. *J. Am. Chem. Soc.* **2009**, *131*, 17552.
(14) Askevold, B.; Khusniyarov, M. M.; Herdtweck, E.; Meyer, K.; Schneider, S. *Angew. Chem. Int. Ed.* **2010**, *49*, 7566.
(15) Friedrich, A.; Drees, M.; Kass, M.; Herdtweck, E.; Schneider, S. *Inorg. Chem.* **2010**, *49*, 5482.
(16) Meiners, J.; Schiebel, M. G.; Lemee-Cailleau, M.-H.; Mason, S. A.; Boeddinghaus, B.; Fassler, T. F.; Herdtweck, E.; Khusniyarov, M. M.; Schneider, S. *Angew. Chem., Int. Ed.* **2011**, *50*, 8184.
(17) Feller, M.; Diskin-Posner, Y.; Shimon, L. J. W.; Ben-Ari, E.; Milstein, D. *Organometallics* **2012**, *31*, 4083.
(18) Askevold, B.; Nieto, J. T.; Tussupbayev, S.; Diefenbach, M.; Herdtweck, E.; Holthausen, M. C.; Schneider, S. *Nat. Chem.* **2011**, *3*, 532.
(19) Scheibel, M. G.; Askevold, B.; Heinemann, F. W.; Reijerse, E. J.; Bruin, B. D.; Schneider, S. *Science* **2012**, *4*, 552.
(20) Fryzuk, M. D.; MacNeil, P. A. *Organometallics* **1983**, *2*, 682.
(21) Fryzuk, M. D.; MacNeil, P. A. *Organometallics* **1983**, *2*, 355.
(22) Fryzuk, M. D.; MacNeil, P. A.; Rettig, S. J. *Organometallics* **1985**, *4*, 1145.
(23) Fryzuk, M. D.; MacNeil, P. A.; Rettig, S. J. *Organometallics* **1986**, *5*, 2469.
(24) Fryzuk, M. D.; MacNeil, P. a.; Rettig, S. J. *J. Am. Chem. Soc.* **1987**, *109*, 2803.
(25) Fryzuk, M. D.; Montgomery, C. D.; Rettig, S. J. *Organometallics* **1991**, *10*, 467.
(26) Maire, P.; Büttner, T.; Breher, F.; Le Floch, P.; Grützmacher, H. *Angew. Chem., Int. Ed.* **2005**, *44*, 6318.
(27) Mikhailine, A. A.; Maishan, M. I.; Lough, A. J.; Morris, R. H. *J. Am. Chem. Soc.* **2012**, *134*, 12266.
(28) Prokopchuk, D. E.; Morris, R. H. *Organometallics* **2012**, *31*, 7375.
(29) Sonnenberg, J. F.; Coombs, N.; Dube, P. A.; Morris, R. H. *J. Am. Chem. Soc.* **2012**, *134*, 5893.
(30) Guan, Z.; Marshall, W. J. *Organometallics* **2002**, *21*, 3580.
(31) Keim, W.; Killat, S.; Nobile, C. F.; Paolo, G.; Englert, U.; Wang, R.; Mecking, S.; Schroder, D. L. *J. Organomet. Chem.* **2002**, *662*, 150.
(32) Dahlenburg, L.; Götz, R. *Eur. J. Inorg. Chem.* **2004**, *2004*, 888.
(33) Batsanov, S. S. *Inorg. Mater.* **2001**, *37*, 871.
(34) Choualeb, A.; Lough, A. J.; Gusev, D. G. *Organometallics* **2007**, *26*, 5224.
(35) Smidt, S. P.; Pfaltz, A.; Martínez-Viviente, E.; Pregosin, P. S.; Albinati, A. *Organometallics* **2003**, *22*, 1000.
(36) Wang, H. H.; Pignolet, L. H. *Inorg. Chem.* **1980**, *19*, 1470.
(37) Chodosh, D. F.; Crabtree, R. H.; Felkin, H.; Morehouse, S.; Morris, G. E. *Inorg. Chem.* **1982**, *21*, 1307.
(38) Xu, Y.; Celik, M. A.; Thompson, A. L.; Cai, H.; Yurtsever, M.; Odell, B.; Green, J. C.; Mingos, D. M. P.; Brown, J. M. *Angew. Chem., Int. Ed.* **2009**, *48*, 582.
(39) Crabtree, R. H.; Felkin, H.; Morris, G. E. *J. Organomet. Chem.* **1977**, *141*, 205.
(40) Ohno, K.; Tsuji, J. *J. Am. Chem. Soc.* **1968**, *90*, 99.
(41) Doughty, D. H.; Pignolet, L. H. *J. Am. Chem. Soc.* **1978**, *100*, 7083.
(42) Saunders, M.; Kates, M. R. *J. Am. Chem. Soc.* **1978**, *100*, 7083.
(43) Anderson, M. P.; Casalnuovo, A. L.; Johnson, B. J.; Mattson, B. M.; Mueting, A. M.; Pignolet, L. H. *Inorg. Chem.* **1988**, *27*, 1649.
(44) Iwai, T.; Fujihara, T.; Tsuji, Y. *Chem. Commun.* **2008**, 6215.

(45) Roa, A. E.; Salazar, V.; Lopez-Serrano, J.; Onate, E.; Paneque, M. *Organometallics* **2012**, *31*, 716.
(46) Ho, H.-A.; Manna, K.; Sadow, A. D. *Angew. Chem., Int. Ed.* **2012**, *51*, 8607.
(47) Yang, X.; Hall, M. B. *J. Am. Chem. Soc.* **2010**, *132*, 120.
(48) Zeng, G.; Li, S. *Inorg. Chem.* **2011**, *50*, 10572.
(49) Li, H.; Wang, X.; Huang, F.; Lu, G.; Jiang, J.; Wang, Z.-X. *Organometallics* **2011**, *30*, 5233.
(50) Sandhya, K. S.; Suresh, C. H. *Organometallics* **2011**, *30*, 3888.
(51) Yang, X. *ACS Catal.* **2012**, *2*, 964.
(52) Ma, C.; Piccinin, S.; Fabris, S. *ACS Catal.* **2012**, *2*, 1500.
(53) Li, H.; Wen, M.; Wang, Z.-X. *Inorg. Chem.* **2012**, *51*, 5716.
(54) Herde, J. L.; Lambet, J. C.; Senoff, C. V. *Inorg. Synth.* **1974**, *15*, 18.